Phys Chem Minerals (2004) 31: 232–239
DOI 10.1007/s00269-004-0379-x

ORIGINAL PAPER

G. V. Gibbs · D. F. Cox · N. L. Ross

A modeling of the structure and favorable H-docking sites and defects for the high-pressure silica polymorph stishovite

Received: 16 June 2003 / Accepted: 23 November 2003

Abstract Employing first-principles methods, the docking sites for H were determined and H, Al, and vacancy defects were modeled with an infinite periodic array of super unit cells each consisting of 27 contiguous symmetry nonequivalent unit cells of the crystal structure of stishovite. A geometry optimization of the super-cell structure reproduces the observed bulk structure within the experimental error when P1 translational symmetry was assumed and an array of infinite extent was generated. A mapping of the valence electrons for the structure displays mushroom-shaped isosurfaces on the O atom, one on each side of the plane of the OSi_3 triangle in the nonbonded region. An H atom, placed in a cell near the center of the super cell, was found to dock upon geometry optimization at a distance of 1.69 Å from the O atom with the OH vector oriented nearly perpendicular to the plane of the triangle such that the OH vector makes a angle of 91° with respect to [001]. However, an optimization of a super cell with an Al atom replacing Si and an H atom placed nearby in a centrally located cell resulted in an OH distance of 1.02 Å with the OH vector oriented perpendicular to [001] as observed in infrared studies. The geometry-optimized position of the H atom was found to be in close agreement with that (0.44, 0.12, 0.0) determined in an earlier study of the theoretical electron density distribution. The docking of the H atom at this site was found to be ~330 kJ mol^{-1} more stable than a docking of the atom just off the shared OO edge of the octahedra as determined for rutile. A geometry optimization of a super cell with a missing Si generated a vacant octahedra that is 20% larger than that of the SiO_6 octahedra. The valence electron density distribution displayed by the two-coordinate O atoms that coordinate the vacant octahedral site is very similar to those displayed by the bent SiOSi angles in coesite. The internal distortions induced by the defect were found to diminish rather rapidly with distance, with the structure annealing to that observed in the bulk crystal to within about three coordination spheres.

Keywords Spectral studies · Diffraction methods · Super cell structure

G. V. Gibbs (✉) · N. L. Ross
The Department of Geosciences,
Materials Science and Engineering and Mathematics
Virginia Tech, Blacksburg,
VA 24061, USA
e-mail: gvgibbs@vt.edu

D. F. Cox
The Department of Chemical Engineering,
Virginia Tech, Blacksburg,
VA 24061, USA

Introduction: spectral and diffraction studies

In an important infrared spectral study of the hydroxyl contents of accessory minerals in mantle and related rocks, Rossman and Smyth (1990) established that rutile, TiO_2, recovered from mantle eclogites not contains only significant amounts of Al, Fe, Cr and Nb but also comparable amounts of structural OH. In a neutron and X-ray diffraction study of one of the crystals, Swope et al. (1995) concluded on the basis of features in difference density maps that H is located at (0.42, 0.5, 0.0), ~0.25 Å from the OO-shared edge of the TiO_6 octahedra at a distance of 1.04 Å from one of the oxygen atoms such that OH dipole vector is oriented nearly perpendicular to [001] (Fig. 1a). As stishovite has the same crystal structure as rutile, Smyth et al. (1995) concluded that an H atom in stishovite containing trace amounts of H would most likely dock just off the shared edge of the SiO_6 octahedra such that the OH vector is likewise oriented perpendicular to [001]. As stishovite is believed to be an abundant phase in silica-rich regions of the mantle at depths in the Earth in excess of 300 km, Pawley et al. (1993) undertook a high-pressure study of the silica polymorph to see whether OH can be incorporated in the structure in significant amounts as reported for

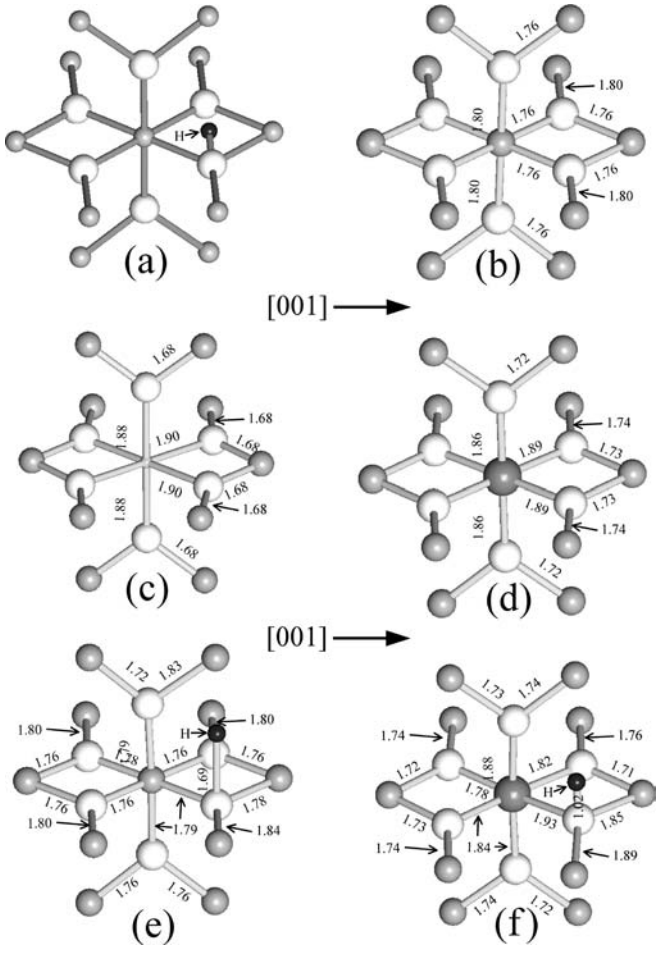

Fig. 1 **a** A representative moiety of the structure of H-bearing rutile displaying a central TiO_6 octahedron with each oxygen atom coordinated by three Ti atoms. The position of the H atom displayed in the figure was determined by Swope et al. (1995) to be nearly in the plane of the shared edge at a distance of 1.04 Å from the oxygen atom and 1.52 Å from two Ti atoms. (see below for the details of this figure and the remaining ones). **b** A moiety of the geometry-optimized super cell structure of stishovite (Fig. 2) displaying a central SiO_6 octahedron with each oxygen atom coordinated by three Si atoms. **c** A vacant vO_6 moiety of the geometry optimized super cell of the stishovite with a vacancy, *v* located at the center of the cell. **d** An AlO_6 moiety of the geometry-optimized stishovite super cell with the Al atom located at the center of the super cell. **e** Geometry-optimized moiety of structure with an H defect. **f** Geometry-optimized Al, H moiety of the cell; the cell was optimized starting with Al at the center of the super cell and with the H atom placed near by at the position determined by Swope et al. (1995). The *white spheres* represent O, the *gray spheres* of intermediate size in **a** represents Ti and Si in **b** and **e**, the *large gray spheres* represent Al in **d**, **f**, the *small gray sphere* in **c** represents a vacancy and the *small black sphere* in **a**, **e** and **f** represents H. The [001] for each of moiety runs *from left to right* with [310] oriented nearly perpendicular to the figure. The bond lengths listed along the bond paths are given in Å. The geometry-optimized super unit cell structures displayed by **c**, **d**, **e**, and **f** were completed with their unit-cell dimensions clamped at the geometry-optimized values (Fig. 2). Even though the point-group symmetry of the super cell was assumed in the calculations to possess C_1, the point symmetries of the moieties displayed in **b**, **c** and **d** each exhibit D_{2d} point symmetry

H-bearing rutile. In an examination of this proposal, they completed a synthesis of stishovite in the system SiO_2–Al_2O_3–H_2O and found that the H content of the resulting crystals is dependent upon their Al content, attaining a maximum value of 550 H atoms per 10^6 Si atoms for an Al_2O_3 content of 1.5 wt%. Using polarized Fourier transform infrared (FTIR) spectroscopic methods, they also found that the greatest absorption of the FTIR spectra occurs when the electric vector **E** is oriented perpendicular to [001] with little or no absorption when it parallels [001]. On the basis of the spectral evidence, Pawley et al. (1993) concluded that the position of the H atom in stishovite is the same as it is in rutile (Smyth et al. 1995); but, with a close scrutiny of the spectra, it is not clear whether or not there is also a small absorption of **E** parallel to [001]. However, Chung and Kagi (2002) have since obtained spectra for a much more water-rich specimen that indicates that there is absolutely no absorption with **E** parallel to [001]. Accordingly, it was concluded that the corresponding OH dipole vector must be strongly constrained to be perpendicular to [001] with little or no scatter in its orientation.

Despite the good agreement between the orientation of the OH vector and the spectral data, a problem exists with the proposed structure of H-bearing stishovite (Smyth et al. 1995). The site that Swope et al. (1995) determined for H-bearing rutile places the H atom equidistant from two Ti atoms. As the separation between the H and each of these atoms is substantially smaller (1.52 Å) than the observed TiH bond length (1.76 Å), a question arises about the stability of such a structure given the strong antibonding interactions that can be expected to obtain between such closely spaced atoms. The location of the H atom in H-bearing stishovite (Smyth et al. 1995), based on the position of H in H-bearing rutile, likewise raises a question of stability given the unusually short contacts between Si and H.

In a recent study of the electron localization function, ELF, and the Laplacian of the theoretical electron density distribution, $-\nabla^2\rho$, Gibbs et al. (2003) and Ross et al. (2003) determined regions in stishovite where the distribution is localized and locally concentrated as local maxima. On the basis of these features, they asserted that H would most likely dock in the vicinity of maxima located 0.96 Å from the O atom. The resulting docking site was considered a favorable location for H not only because it results in an OH vector that is perpendicular to [001], but also because it avoids the short SiH contacts encountered in the earlier modeling of the structure. The goal of this study was to complete first-principles calculations on a super cell (C_1 point symmetry) of the stishovite structure consisting of 54 Si atoms and 108 O atoms to verify and establish the docking site of an H atom in Al-free and Al-bearing stishovite and to compare the results with those proposed on the basis of features displayed by the electron density distribution. It was also of interest to establish the distortions impacted on the structure by the replacement of Si by Al, by an interstitial H atom and by a vacant octahedron.

Localization and local concentration of electron density studies

In stishovite, each oxygen atom is bonded to three silicon atoms forming an OSi_3 triangle about O with all four atoms lying in a common plane. Observed model multipole deformation electron density $\Delta\rho$ maps generated for the structure (Spackman et al. 1987; Kirfel et al. 2001) display peaks along each of the SiO bond vectors at a distance of ~0.45 Å from the oxygen atom. These peaks define where the electron density is localized along the SiO bond vectors. In addition, a peak occurs on each side of the oxygen atom on opposite sides of the plane formed by OSi_3 triangle at a distance of ~0.40 Å. These peaks have been ascribed to localized domains of lone-pair electron density in the nonbonded region of the atom (Spackman et al. 1987). In addition, a mapping of the valence electron density distribution calculated for stishovite display mushroom-shaped isosurfaces likewise displayed on opposite sides of the triangle next to the O atom (Gibbs et al 2003). Such features define sites of potential electrophilic attack, sites favorable for the docking an H atom (cf. Gillespie 1970, Bader et al. 1984; MacDougall 1989). In addition, a mapping of the ELF displays similar features (Gibbs et al. 2001, 2002, 2003a). The maps show that each oxide atom in the silica polymorph is surrounded by five isosurfaces, one located along each of the SiO bond vectors and the remaining two centered on opposite sides of the OSi_3 triangle next to the atom as displayed by the $\Delta\rho$maps. Assuming that H prefers to bond to the atom in the vicinity of its lone-pair electrons, the position of the hydrogen at 0.44, 0.12, 0.0 was established by walking along the vector that radiates from the oxygen atom through the maximum enclosed by the isosurface in the ELF maps a distance of 0.96 Å from the atom. This placed the H atom at a distance of 2.07 Å from the two Si atoms such that the OH vector lies in the 001 plane and makes an angle of 82.3° to [110]. Rather than residing just off the shared edge of the SiO_6 octahedra, the predicted position of the H atom resides in stishovite at a distance of 0.96 Å from the oxygen atom of the OSi_3 triangle such that the OH vector is perpendicular to [001]. The resulting docking site for the H atom not only conforms very nicely with the Pawley et al. (1993) and Chung and Kagi (2002) FTIR measurements, but it also avoids a short SiH contact compared with the SiH bond length (1.48 Å). Further, on the basis of a mapping of the (3,−3) critical points of $-\nabla^2\rho$ for stishovite, Ross et al. (2003) obtained a similar position for the H atom.

Proposed study

The determination of the position of H in a stishovite crystal containing trace amounts of H by diffraction methods can be a difficult and daunting task, particularly when given that experimental difference maps are not series termination error-free, with maxima and minima commonly being developed in the regions between the highly scattering atoms. Indeed, the minima observed in the neutron difference density maps between the Ti atoms in rutile and ascribed to H may instead reflect a feature related to series-termination error. Further, the determination of the distortions in stishovite about defect H and Al atoms or a vacancy can be a difficult if not an impossible undertaking in a crystal-structure analysis. However, since first-principle calculations completed for quartz (Gibbs et al. 1999) and coesite (Gibbs et al. 2000) have generated model structures for these silica polymorphs that rival the accuracies of the structures observed for a range of pressures, we have undertaken similar calculations for stishovite; but rather than completing bulk crystal calculations as done for quartz and coesite, we have undertaken calculations for an infinite periodic array of super unit cells of the structure each consisting of 27 contiguous nonequivalent unit cells of stishovite. With such a super- cell model, H and Al defect atoms and a vacancy can be introduced in a cell at or near the center of the cell and the resulting structure geometry optimized. This provides a strategy not for only determining the docking position of an H defect but also for determining the distortions of the structure about the defect as well as the distortions of the structure about an Al defect and a vacancy. The resulting structure of the super cell will also provide us with information pertaining to the impact of the defects on the overall structure of the cell, shedding light on whether or not the effect of the defect dies rapidly with distance. Given that neutral H and Al atoms were introduced as defects and a neutral Si atom was removed in creating a vacancy, each supercell was necessarily optimized assuming electrostatic neutrality.

In accomplishing our goal, the structures of five different model super unit cells were geometry optimized in this study: (1) a defect-free super cell representing the bulk structure of stishovite, (2) a cell with a missing Si atom at its center, (3) an cell with an Al atom replacing the central Si atom, (4) a cell with a defect H atom in the central cell, and (5) a cell with Al replacing the central Si atom with an accompanying H atom located at the position proposed by Smyth et al. (1995). The distribution of the valence electrons was evaluated for each of the structures in an exploration of the connection between potential docking sites of H and domains of lone pair electron density.

Computational strategy

The calculations were performed with VASP, a periodic plane wave density functional code (Kresse and Hafner 1993; Kresse and Furthmuller 1996a, b), utilizing ultrasoft pseudopotentials (Vanderbilt 1990) and the local density approximations (LDA) to account for the exchange correlation to the total energy. The kinetic energy cutoff and the density of the Monkhorst–Pack k-point mesh (Monkhorst and Pack 1976) were chosen to be large enough to ensure convergence of the geometry-optimized structure and energy. The bulk stishovite structure was modeled with a 162-atom super unit cell consisting of a 3 × 3× 3 array of primitive (two Si

and four O atoms each) cells. As observed above, the large super cell was used so that the vacancies and impurities could be isolated within the extended periodic structure. For the geometry optimization, the unit-cell dimensions were fixed at the zero pressure values determined for the bulk structure within the LDA and the coordinates of the atoms within the cell were varied assuming C_1 point symmetry until the component forces on all of the atoms were small, less than $0.03\,\mathrm{eV\,\AA^{-1}}$. For the geometry-optimized structures, the electron localization function and the valence electron density distribution were determined with the VASP software, and figures of the isosurfaces were generated with a modified version of the desktop 3 D visualization software of Terriberry et al. (2002).

Optimized super cell structure; A comparison with the observed structure

The geometry-optimized defect-free super cell representation of the stishovite structure is displayed in Fig. 2. The observed SiO_6 octahedron in stishovite consists of two equivalent apical bonds of length 1.808 Å and four shorter equivalent equatorial SiO bonds of length 1.757 Å (Kirfel et al. 2001), bond lengths that are in close agreement with those generated for the super cell structure [1.801 Å (2x), 1.761 Å (4x) (Fig. 1b]. As expected, for the observed bulk structure the edges of the octahedron that are shared with adjacent octahedra are significantly shorter (2.29 Å) than the remaining ten unshared edges, eight of which are equivalent with edge lengths of 2.52 Å and two are equivalent with lengths of 2.67 Å. The OO separations generated for the structure agree with those observed within 0.01 Å, on average, and the OSiO angles agree within 0.2°. The average SiO bond lengths for the observed and the super cell structures are both 1.74 Å while the volume of the SiO_6 octahedron ($7.360\,\mathrm{\AA^3}$) for the observed structure is slightly larger than that displayed by the super cell structure ($7.356\,\mathrm{\AA^3}$). On the other hand, the values of the mean octahedral quadratic elongations calculated for the octahedra of both structures are identical (1.008), evidence that the distortions in both structures are virtually identical (Robinson et al. 1971). Moreover, the D_{2h} point symmetry of the Si and the C_{2v} point symmetry of the O atoms of the representative unit is preserved with the bond length and angles on the periphery of the super unit cell matching those on the interior, despite the assumption of C_1 point symmetry in the calculations. Clearly, the VASP software does an excellent job in reproducing the observed structure of stishovite.

A calculation of the ELF distribution for the structure displays isosurfaces localized along each of the SiO bond vectors and in the lone -pair region of each oxygen atom as reported (Fig. 3) earlier for stishovite (Gibbs et al. 2001, 2003). The valence electron density distribution, ρ, evaluated for the defect super cell of stishovite is virtually identical with that calculated for the bulk crystal. As observed earlier by Gibbs et al. (2003), each O atom is coordinated by two mushroom-shaped isosurfaces (Fig. 4a) located on opposite sides of the OSi_3 triangle. As these features lie in the nonbonded region of the O atom, they can be ascribed to domains of the lone-pair electron density. Moreover, they constitute sites where H can be expected to dock such that the OH vector is perpendicular to [001].

A super cell with an octahedral vacancy, v

A representative moiety of the structure about the missing central Si atom in the geometry-optimized super cell is displayed in Fig. 1c. As expected, with the missing Si atom, the structure about the vacancy, *v*, is dilated

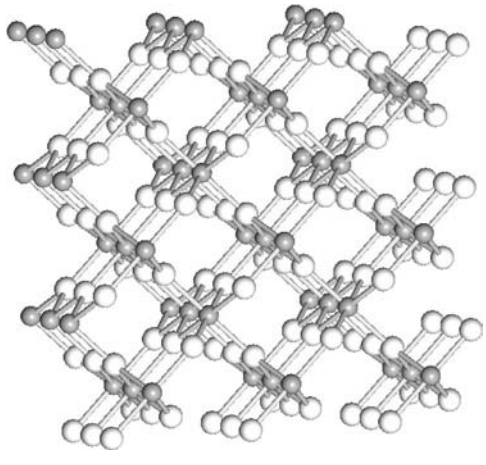

Fig. 2 A drawing of the atoms comprising a super unit cell consisting of 27 nonequivalent stishovite unit cells, 54 nonequivalent Si atoms (*gray spheres*), and 108 nonequivalent O atoms (*white spheres*). The structure is viewed 10° off [001] and displays square channels enclosed by OSi_3 triangles. The *gray lines* that connect the Si and O atoms represent the bond paths between Si and O. The geometry-optimized unit-cell dimensions are $a = b = 12.462$ A, $c = 8.001$ A, $\alpha = \beta = \gamma = 90.0°$

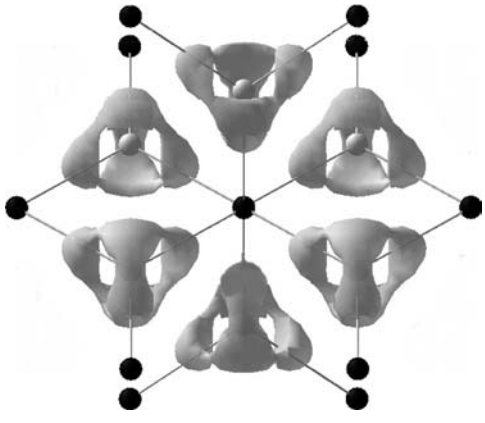

Fig. 3 A map of an electron localization function envelope for the moiety displayed in Fig. 1b calculated at an ELF value of 0.832. The *light gray spheres* represent O and the *black ones* represent Si. Each O atom is coordinated by three Si atoms forming a triangular OSi_3 with all four atoms lying in a common plane. The ELF envelopes extend along each of the SiO bonds of the triangle and into the lone-pair region of the O atom on opposite sides of the triangle. By extending a vector from the O atom through the maximum of the ELF in the lone-pair region a distance of 0.96 Å, Gibbs et al. (2003) located a favorable docking site for the H atom at (0.44, 0.12, 0.0)

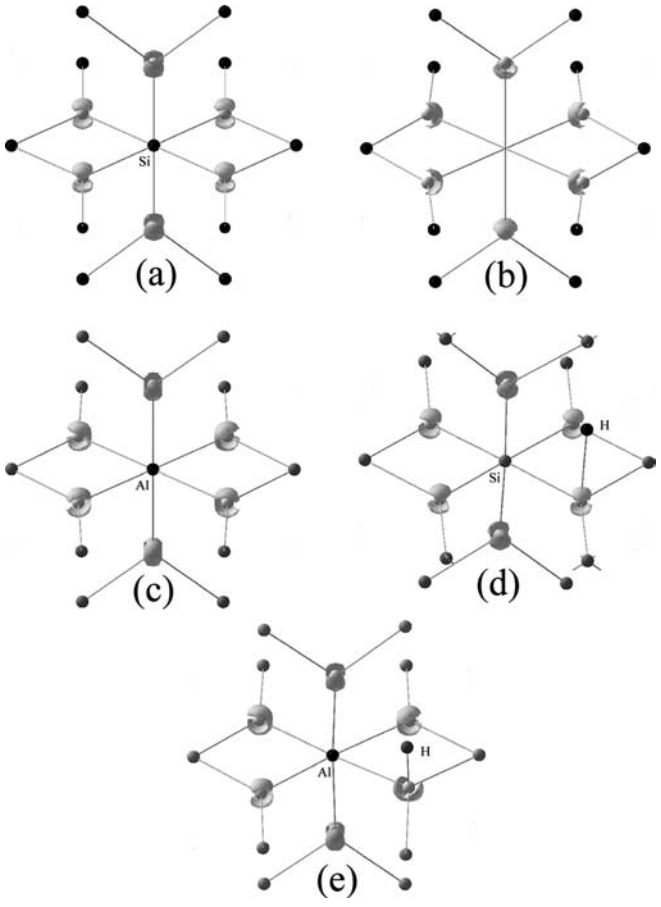

Fig. 4a–e Moieties of the structure of stishovite displaying the valence electron density isosurfaces calculated at the 6.82 $Å^{-3}$ level. Isosurfaces displayed **a** for the SiO_6 octahedron depicted in Fig. 1b; **b** for the vacancy depicted in Fig. 1c; **c** for the AlO_6 octahedron depicted in Fig. 1d; **d** for SiO_6 octahedron and H depicted in Fig. 1 **e** for the AlO_6 octahedron and H depicted in Fig. 1f. The *light gray spheres* represent O

such that the volume (8.936 $Å^3$) of the resulting vO_6 octahedron is ~20% larger than that for the SiO_6 octahedra in stishovite. The distances between the nearest-neighbor oxygen atoms and the vacancy range between two at 1.88 Å and four at 1.90 Å, where the smaller distances involve the apical atoms and the longer ones the equatorial atoms of the octahedron. This is unlike the SiO_6 octahedra in both the super cell and observed stishovite structures where the longer SiO bonds (1.80 Å) involve the apical oxygen atoms and the shorter ones (1.76 Å) involved the equatorial atoms. In other words, the situation is reversed for the vacant octahedron, where the distances between the vacancy and the apical atoms are smaller than those between with vacancy and the equatorial atoms. The edges shared between the vacant octahedra and the Si-containing one are shorter (2.45 Å) than the unshared ones of the vacancy [2.67 Å (8x), 2.91 Å (2x)]. It is noteworthy that the local point symmetry of the vacant octahedron is D_{2h} as observed for the SiO_6 coordination polyhedron in stishovite. The bond lengths of the SiO_6 octahedra in the second coordination sphere from the vacancy are distorted by 0.01 Å, on average, from those generated for the representative unit displayed in Fig. 1b while those of the third coordination sphere are distorted only by 0.005 Å, on average. The angles in the coordination sphere likewise show little distortion. Hence, the presence of a vacancy distorts the local environment by introducing relatively large distortions in the structure within the radius of the second coordination sphere (~5 Å). Accordingly, the effect of the vacancy is relatively short-ranged with little or no distortions imposed on the structure in the third coordination sphere which is at a radius of ~10 Å from the vacancy. However, the bond lengths about the first coordination sphere of the vO_6 polyhedron are more highly distorted than the remaining bonds of the structure. These bonds involve the O atoms that coordinate the vacant site. Because of the vacancy, these atoms are bonded to only two Si atoms and as such the SiO bonds involving these atoms are significantly shorter (1.68 Å) than those involving the atoms bonded to three Si atoms (1.79 Å).

The O atoms that coordinate the octahedral vacancy are each two-coordinated like those in coesite. A mapping of the valency electron density distribution for the bent SiOSi angles in coesite shows that a crescent-shaped isosurface caps the O atom at the apex of the angle and wraps about halfway around the atom. The distribution of valence electrons for the two coordinate O atoms of the vacancy is also crescent shaped (Fig. 4b). With this configuration of lone-pair domains, a docking of an H atom in the vicinity of a vacancy in shishovite may result in OH vectors directed either along [110] or [225] or both. To our knowledge, the FTIR studies that have been completed only find evidence for an OH vector oriented perpendicular to [001]. In the case of coesite, the height of the peak in the valence electron density distribution associated with an O atom was found to depend on the size of the SiOSi angle; the wider the angle, the smaller the peak and the longer the bonded interaction. A similar relationship exists for the SiOSi angles that surround the vacancy. A maximum valence density of 7.44 e$Å^{-3}$ is displayed for the O atom involved in an angle of 102.7° while maximum density of 7.13 e$Å^{-3}$ is displayed for the O atom involved in an angle of 141.0°. This result conforms with the general rule that the narrower the SiOSi angle, the greater the local concentration of the electron density in the lone-pair region, the more nucleophilic the O atom and the more susceptible the atom to electrophilic attack (Gibbs et al. 2001, 2002, 2003a, b; also, see a related argument proposed by Revesz et al. 2000).

A super cell with an Al defect replacing Si

The local structure about the Al atom defect replacing a Si atom in the central cell in the geometry optimized super cell is displayed in Figure 1d. As in the case of the SiO_6 and the vO_6 octahedra, the local point symmetry of

the AlO_6 octahedron is likewise D_{2h}. The bond-length distortions imposed on the structure by the Al atom defect is less than that imposed by the vacancy inasmuch as the volume of the AlO_6 octahedron is only ~10% larger than that for the SiO_6 octahedra. The lengths of the AlO bonds involving the apical oxygen atoms are both longer (1.86Å) than those involving the equatorial atoms (1.84Å) in conformity with the SiO_6 octahedra in stishovite. As the sum of the bond strengths reaching the atoms of the AlO_6 octahedron is less than 2.0, the SiO bonds involving these atoms are shorter (1.73Å), on average, than those bonded to three Si atoms (1.788Å). The bond lengths length are distorted 0.005Å, on average, in the second coordination sphere of octahedra about the AlO_6 with the distortions in the third coordination sphere decreasing to 0.001Å, on average.

The valence electron density map evaluated for the super cell with the Al defect is displayed in Fig. 4c. The ρ isosurfaces displayed about the O atom bonded to two Si and one Al atom wraps about the AlO bond and is localized in the lone-pair region on both sides of the $AlSi_2O$ triangle (Fig. 4c). As the magnitude of the maxima in the lone-pair region is larger than it is for O atoms coordinated by three Si atoms, H can be expected to dock on the O atoms bonded to Al in preference to O bonded to three Si atoms.

A super cell with an interstitial H defect

Running parallel to [001], there exits in the stishovite structure square channels (Fig. 2) bounded on four sides by OSi_3 triangles. Evidence provided by valence, deformation, ELF, and $-\nabla^2\rho$ maps discussed above indicates that domains ascribed to nonbonded electron pairs project into the channels from each oxygen atom. As each triangle comprising the channels is $P4_2/mnm$–equivalent, each oxygen atom is equivalent and an equally favorable site for docking hydrogen. With the H placed at the site proposed by Smyth et al. (1995), it moved upon geometry optimization toward the center of the tube such that it ended up tetrahedrally coordinated with one OH bond at 1.68 Å, one at 1.69 Å and two longer ones at 1.87 Å. The one 1.68 Å in length is displayed in Fig. 1e, where the OH vector makes an angle of ~91° with [001]. The vector is also nearly perpendicular to the OSi_3 triangle; the three SiOH angles are 88.6°, 88.7°, and 90.4°. The oxygen atom in this case lies nearly in the plane of the three coordinating Si atoms in the central cell. The reduction in energy associated with the movement of the H atom from where it was located by Smyth et al. (1995) to its position in Fig. 1e is ~–585 kJ mol^{-1}. In other words, the placement of the H just off the shared OO edge is clearly a destablizing feature of the structure. The SiO bond lengths involving the oxygen atoms bonded to the H are as much as 0.15 Å longer than those in the defect-free bulk structure. However, the effect of the H defect is short-ranged and has little effect on the atoms in the second sphere of nearest neighbors.

The valence electron density isosurface map for the H defect shows that the H docks directly above the lone-pair domain on the O atom of the Si_3O triangle as expected (Fig. 4d). The domain between the O atom and the H is slightly smaller in magnitude (7.22 eÅ^{-3}) than the remaining domains in structure (7.35 eÅ^{-3}). As shown below, with the replacement of the SiO_6 octahedron in the structure by an AlO_6 octahedron, the H atom docks 1.02 Å from the O atom and the lone-pair domain between the H and the O atom is missing (Fig. 4e).

A super cell with Al atom replacing Si and an interstitial H atom

The super cell with an Si atom replaced by Al with an interstitial H atom in the central cell was constructed by replacing the central Si atom by Al and placing the H atom at the position proposed by Swope et al. (1995) for the H atom in H-bearing rutile (Fig. 1a). Upon geometry optimization, the H atom migrated to a position directly above the O atom of the Si_3O triangle at a distance of 1.02 Å, as displayed in Fig. 1f. The decrease in energy accompanying the geometry optimization of the structure was ~330 kJ mol^{-1}. Thus, the location of the H in close contact with Si and Al is a destablizing feature and an unfavorable position for H. The OH vector makes an angle of 93° with respect to [001] in the geometry-optimized structure, close to that predicted on the basis of the position of the lone-pair features (Gibbs et al. 2003; Ross et al. 2003). An examination of the geometry of the moiety displayed in Fig. 1f shows, as expected, that the AlOH and SiOH bond lengths are substantially longer (1.93, 1.87 Å, respectively), than the AlO and SiO bond lengths (1.83, 1.73 Å, respectively). Unlike the O atom in stishovite, which lies in the triangular plane formed by the three coordinating Si atoms, it is displaced off the plane ~0.15 Å such that $<$ AlOH = 98.2°, $<$ SiOH = 101.1°, and $<$ SiOH = 89.9° rather than 90.0° as observed for stishovite (Fig. 1f). The lengths of the SiO bonds involving the oxygen atoms of the AlO_6 octahedron are ~0.05 Å shorter than those observed for stishovite. These distortions about the defect diminished rapidly from the AlO_6 octahedron, with the bond lengths in the third coordination sphere matching those observed for stishovite.

As observed above, the docking of a H at 1.02 Å from the oxide anion is accompanied by a redistribution of the valence electron density distribution ascribed to the lone-pair domain into both the binding region along the AlO bond and the antibonding region at the backside of the Al (Fig. 4e). The redistribution of ρ into the antibonding region may account for why the length (1.93 Å) of the AlO bond involving the O atom is the longest bond in the AlO_6 octahedron.

Summary

The spatial distribution of the lone-pair electron density distribution provides a basis for understanding where the H atom favorably docks in the silica polymorphs. In the case of H-bearing coesite, the lone-pair features correspond with the docking positions determined in a careful FTIR study (Koch–Muler et al. 2002) with the protons preferring the oxygen atoms involved in bent angles and avoiding those involved in wide angles. In the case of H–bearing stishovite, the proton also docks in the vicinity of lone-pair electrons such that the OH vector is nearly perpendicular to [001] as found in FTIR studies (Pawley et al. 1993; Chung and Vagi 2002). It is noteworthy that the OH vector is established to be nearly perpendicular to [001] with or without the presence of an Al atom, but clearly an OH vector of magnitude 1.69 Å cannot explain the spectra. Clearly, the presence of Al together with the H with an OH vector with a magnitude of 1.01 Å can explain the spectra as concluded in the spectral studies. Finally, when used in conjunction with spectral methods, a knowledge of the spatial distribution of the domains of lone-pair electrons as generated by theoretical strategies can be expected to be an important auxiliary tool for establishing the docking sites of H and other defect atoms in a material.

Acknowledgements The National Science Foundation (grants EAR–9627458, GVG and M. B. Boisen, Jr. and EAR–0229472, N. L. Ross, and GVG), The Chemical Sciences, Geosciences and Biosciences Division, Office of Basic Energy Sciences, Office of Science, US, Department of Energy (grant DE–FG02–97ER14751, DFC) and The US. Department of Energy (grant DE–FG 02–03ER15389, J. D. Rimstidt and GVG) are thanked for generously supporting this study. The study was also supported in part by the National Computational Science Alliance under a SURA Bloack Grant (project ndg) and utilizing the SGI Origin2000 at the National Center for Supercomputing Applications. G.V.G is pleased to thank George Rossman for generously sharing his extensive knowledge about H in rutile and stishovite. This paper was written in part while G.V.G was a Visiting Professor in the Chemistry Department at the University of New England in Armidale, Australia. The Faculty of the Sciences is thanked for awarding him a Visiting Distinguished Professor Scholarship. Professors Mark Spackman and Geoff Ritchie are also thanked for their kind hospitality and for making the visit a very stimulating and worthwhile experience. We are grateful to Monika Kock–Müller and Mauro Principe for their careful and valuable reviews of the manuscript; where their insightful comments and suggestions resulted in substantial improvements. Monika is also thanked for bringing to our attention a number of important references on the IR spectra of stishovite and rutile.

References

Bader RFW, MacDougall PJ, Lau CDH (1984) Bonded and nonbonded charge concentrations and their relation to molecular geometry and reactivity. J Am Chem Soc 106: 1594–1605

Chung JI, Kagi H (2002) High concentration of water in stishovite in the MORB system. Geophys Res Lett 29: 2020

Gibbs GV, Rosso KM, Teter DM, Boisen MB, Bukowinski MST (1999) Model structures and properties of the electron density distribution for low quartz at pressure: a study of the SiO bond. J Mol Struct 13–25: 13–25

Gibbs GV, Boisen MB, Rosso KM, Teter DM, Bukowinski MST (2000) Model structures and electron-density distributions of the silica polymorph coesite at pressure: an assessment of OO-bonded interactions. J Phys Chem (B) 104: 10534–10542

Gibbs GV, Boisen MB, Beverly LL, Rosso KM (2001) A computational quantum-chemical study of the bonded interactions in earth materials and structurally and chemically related molecules, molecular modeling theory: applications in the geosciences. In: Cygan RT, Kubicki JD (eds) Reviews in Mineralogy and Geochemistry, vol. 42 Rosso JJ (Series Ed.) Mineralogical Society of America, Washington, DC 345–382

Gibbs GV, Cox DF, Crawford TD, Boisen MB, Lim M (2002) A mapping of the electron localization function for the silica polymorphs: evidence for domains of electron pairs and sites of potential electrophilic attack. Phys Chem Miner 29: 307–318

Gibbs GV, Cox DF, Boisen MB, Downs RT, Ross NL (2003a) The electron localization function: a tool for locating favorable proton docking sites in the silica polymorphs, Phys Chem Miner 30: 305–316

Gibbs GV, Whitten AE, Spackman MA, Stimpfl M, Downs RT and Carducci MD (2003b) An exploration of theoretical and experimental electron density distributions and SiO bonded interactions for the silica polymorph coesite. J Phys Chem (B) 209(43): 12996–13006

Gillespie RJ (1970) The valence-shell electron pair model of molecular geometry, J Chem Edu 4718–23

Kirfel A, Krane HG, Blaha P, Scwartz K, Lippmann T (2001) Electron-density distribution in stishovite, SiO_2: a high-energy synchrotron radiation study. Acta Crystallogr (A) 57: 663–677

Koch–Müller M, Fei Y, Hauri E, Liu Z (2001) Location and quantative analysis of OH in coesite. Phys Chem Miner 28: 693–705

Kresse G, Hafner J (1993) Ab initio molecular dynamics for liquid metals. Phys Rev (B) 47: 558–561

Kresse G, Hafner J (1994) Ab initio molecular-dynamics simulation of the liquid-metal amorphous-semiconductor transition in germanium. Phys Rev (B) 49: 14251–14269

Kresse G, Furthmüller J (1996a) Efficiency of abinitio total energy calculations for metals and semiconductors using a plane-wave basis set. Comput Mat Sci 6: 15–50

Kresse G, Furthmüller J (1996b) Efficient iterative schemes for ab initio total-energy calculations using a plane-wave basis set. Phys Rev (B) 54: 11169–11186

MacDougall PJ (1989) The Laplacian of the electron charge distribution, PhD Thesis, McMaster University 1–128

Monkhorst HJ, Pack JD (1976) Special points for Brillouin-zone integrations. Phys Rev (B) 13: 5188–5192

Pawley AR, McMillian PF, Holloway JR (1993) Hydrogen in stishovite, with implications for mantle water content. Science 261: 1024–1026

Revesz AG, Stahlbush RE, Hughes HL (2000) Hydrogen in buried SiO_2 layers. In: Massoud HZ, Baumvol IJR, Hirose M, Poindexter EH (eds) The physics and chemistry of SiO_2 and Si–SiO_2 interface, vol. 4. The Electrochemical Society Inc., Pennington, NJ 235–240

Robinson K, Gibbs GV, Ribbs PH (1971) Quadratic elongation: a quantitative measure of the distortion in coordination polyhedra. Science 172567–172570

Ross NL, Gibbs GV, Rosso KM (2003) Potential docking sites of hydrogen in high-pressure silicates. Am Mineral 881452–881459

Rossman GR, Smyth JR (1990) Hydroxly contents of accessory minerals in mantle eclogites and related rocks. Am Mineral 75775–75780

Spackman MA, Hill RJ, Gibbs GV (1987) Exploration of structure and bonding in stishovite via Fourier and pseudoatom refinement methods. A comparison with rutile. Phys Chem Miner 14: 139–150

Smyth JR, Swope RJ Pawley AR (1995) H in rutile-type compounds: II Crystal chemistry of Al substitution in H-bearing stishovite. Am Mineral 80: 454–456

Swope RJ, Smyth JR, Larson AC (1995) H in rutile-type compounds: I Single-crystal neutron and X-ray diffraction study of H in rutile. Am Mineral 80: 448–453

Terriberry TB, Cox DF, Bowman DA (2002) A tool for the interactive 3D visualization of electronic structures in molecules and solids. Comput Chem 26: 313–319

Vanderbilt D (1990) Soft self-consistent pseudopotentials in a generalized eigenvalue formalism. Phys Rev (B) 41: 7892–7895